ELSEVIER

Chemical Engineering Journal 141 (2008) 99–111

Chemical Engineering Journal

www.elsevier.com/locate/cej

Biosorption of hexavalent and trivalent chromium by palm flower (*Borassus aethiopum*)

R. Elangovan [a], Ligy Philip [a,*], K. Chandraraj [b]

[a] *Department of Civil Engineering, Indian Institute of Technology Madras, Chennai 600036, India*
[b] *Department of Biotechnology, Indian Institute of Technology Madras, Chennai 600036, India*

Received 28 February 2007; received in revised form 2 June 2007; accepted 30 October 2007

Abstract

In this paper, results of Cr(VI) and Cr(III) sorption from aqueous phase by palm flower (*Borassus aethiopum*) is presented. Batch kinetic and equilibrium experiments were conducted to determine the adsorption kinetic rate constants and maximum adsorption capacities. Both Cr(III) and Cr(VI) adsorption followed a second-order kinetics. For Cr(III), maximum adsorption capacity was 6.24 mg/g by raw adsorbent and 1.41 mg/g by acid treated adsorbent. In case of Cr(VI), raw adsorbent exhibited a maximum adsorption capacity of 4.9 mg/g, whereas the maximum adsorption capacity for acid treated adsorbent was 7.13 mg/g. There was a significant difference in the concentrations of Cr(VI) and total chromium removed by palm flower. In case of Cr(VI) adsorption, first it was reduced to Cr(III) with the help of tannin and phenolic compounds and subsequently adsorbed by the biosorbent. Acid treatment significantly increased Cr(VI) adsorption capacity of the biosorbent whereas, alkali treatment reduced the adsorption capacities for Cr(VI). However, in case of Cr(III), acid treatment significantly reduced the adsorption capacity whereas the adsorption capacity of alkali treated biosorbent was slightly less than that of raw adsorbent. FT-IR spectrum showed the changes in functional groups during acid treatment and biosorption of Cr(VI) and Cr(III). Column studies were conducted for Cr(III) to obtain the design parameters require for scale-up.

Keywords: Biosorption; Hexavalent chromium; Reduction; Column study; Equilibrium models; Palm flower; Regeneration; Trivalent chromium

1. Introduction

Pollution by heavy metals has received major attention in the recent years due to its toxicity and wide spread occurrence. Chromium is one such heavy metal being in use in various industrial applications like tanning, metallurgy, plating and metal finishing. Chromium exists in two stable oxidation states, Cr(III) and Cr(VI), in nature. The trivalent form is relatively innocuous, but hexavalent chromium is toxic, carcinogenic and mutagenic in nature, highly mobile in soil and aquatic system and also is a strong oxidant capable of being adsorbed by the skin [1].

Of the various treatment techniques available for chromium removal, the most commonly used ones are adsorption, reduction and precipitation, ion exchange and reverse osmosis. Among these methods, adsorption is found to be simple, cost effective and a versatile method for removing heavy metals [2]. In addition, adsorption can remove heavy metals to a lower level than precipitation over a wide range of pH. A number of natural and synthetic adsorbents have been studied by various researchers [3–5] for the removal of heavy metals.

Sorption of heavy metals onto biosorbents is proved to be an attractive method due to the availability of large surface area, selective adsorption of metal ions and possible operation over a broad range of environmental conditions [6]. Variety of biosorbents, including microorganisms have been tried for the removal of heavy metals from aqueous solution [7–12], including algae [13] plant biomass [14,15] agricultural byproducts [16], beech sawdust [17] eucalyptus bark [3] seaweeds [18,19] coir pith, peanut husks carbon [4] palm pressed leaves [20] agro waste [2], etc.

Romero-González et al. [21] reported Cr(III) biosorption onto *Agave lechuguilla.* Biosorption of Cr(III) was due to interactions with surface carboxyl groups of the biosorbent's cell tissue. Park et al. [22] also used brown seaweed, *Ecklonia* sp., for

* Corresponding author. Tel.: +91 44 22574274; fax: +91 44 22574252.
E-mail address: ligy@iitm.ac.in (L. Philip).

1385-8947/$ – see front matter © 2007 Elsevier B.V. All rights reserved.
doi:10.1016/j.cej.2007.10.026

Nomenclature

A_r	constant of Redlich–Peterson isotherm $(L/mg)^{b_r}$
A_t	constant of Toth isotherm (L/mg)
b	Langmuir adsorption constant (L/mg)
b_r	constant of Redlich–Peterson isotherm
C_b	Breakthrough metal ion concentration (mg/L)
C_e	residual concentration at equilibrium (mg/L)
k_1	first-order rate constant
k_2	pseudo-second-order rate constant
K_a	rate constant (L/mg h)
K_F	Freundlich adsorption constant $(mg/g)/(mg/L)^n$
K_r	constant of Redlich–Peterson isotherm (L/g)
K_{RP}	constant of Radke–Prausnitz isotherm (L/g)
K_s, m_s	empirical parameter (Sips models)
K_t	constant of Toth isotherm (mg/g)
^{m}RP	constant of Radke–Prausnitz isotherm
n	Freundlich adsorption constant
N_0	sorption capacity of bed (mg/L)
q_e	adsorbed quantity per gram of biomass (mg/g)
q_m	maximum specific uptake corresponding to sites saturation (mg/g)
T	constant of Toth isotherm
t	the contact time (h)
v	the linear velocity (cm/h)

biosorption of Cr(VI). When wastewater containing Cr(VI) was placed in contact with this biomass, the Cr(VI) was completely reduced to Cr(III). The converted Cr(III) either appeared in solution or was partly bound to the biomass. Romero-González et al. [23] investigated Cr(VI) biosorption using *Agave lechuguilla*. Cr(VI) binding by *A. lechuguilla* at pH 2.0 was due to either electrostatic attraction of Cr(VI) oxyanions by positively charged ligands such as protonated amines or through reduction of Cr(VI) to Cr(III), and subsequent binding of Cr(III) to the biomass.

While selecting the biosorbent, its availability, cost of production, and other beneficial uses have to be taken into account. Palm flower (male) is an inexpensive and abundant material which does not have any other reported beneficial use. As per our knowledge, no studies are available in the literature describing the potential of palm flower for removing chromium from aqueous solution. Moreover, the mechanism of Cr(VI) sorption by many biosorbents are yet to be elucidated. The objective of this study was to evaluate the potential of a natural biosorbent, palm flower *Borassus aethiopum*, a widely available natural material, in sorbing Cr(III) and Cr(VI) from aqueous solution. For this, batch and laboratory scale flow experiments were conducted. Attempt was also made to understand the mechanism of chromium sorption on palm flower.

2. Materials and methods

2.1. Preparation of raw biosorbents

Palm flower (*B. aethiopum*) collected from IIT Madras Campus, Chennai was washed thoroughly with distilled water and dried at 60 °C for 48 h in an oven. The biosorbent was then cut into small pieces, ground in a blender and sieved to obtain constant size particles (between 400 and 500 μm).

2.2. Treatment with acid and alkali

4N H_2SO_4/NaOH solutions were used for pre-treating the raw biosorbents. For this, 10 g of raw adsorbent was mixed with 100 mL of acid and alkali solution and agitated at 150 rpm for 24 h. The biosorbent was then washed thoroughly with distilled water until the pH reached nearly neutral (7 ± 0.5) and then dried at 60 °C for 24 h.

2.3. Batch sorption experiments

Batch kinetic experiments were conducted in 250 mL conical flasks with a working volume of 100 mL. 1 g of biosorbent was added to 100 mL of 25 mg/L Cr(III) solution with an initial pH of 4.5. The flasks were agitated on a rotary shaker at 150 rpm and 30 °C. Samples were collected at different time intervals, centrifuged and analyzed for residual Cr(III) and COD concentrations. Isotherm studies were performed by varying the initial chromium concentrations from 10 to 150 mg/L at a pH of 4.5. Sorption studies for Cr(VI) also were conducted in the same manner.

2.4. Desorption studies

Desorption studies were carried out using 5N H_2SO_4. For this, 1 g of exhausted adsorbent was taken in a 250 mL conical flask, mixed with 100 mL of 5N H_2SO_4 solution and agitated in a shaker at 150 rpm for 3 h. Desorbed Cr(III) concentration was estimated with respect to time by analyzing the released Cr(III) concentration in the sample. All the above experiments were also carried out with Cr(VI). Once desorption attained the equilibrium, the adsorbent was washed several times with distilled water in order to remove excess acid. It was again used as an adsorbent in more cycles to evaluate the reuse potential of the sorbent.

2.5. Quantification and chromium reduction potential of released pigments

Pigment extraction experiments were carried out by agitating 500 mg of adsorbent in 100 mL of eluent in a 250 mL conical flask for 4 h. Distilled water, phosphate buffer (100 mM) and ethanol were used as eluents. The adsorbent and adsorbate were separated by centrifuging at $8000 \times g$ for 5 min. The pigment released was measured in terms of COD. Concentrations of tannin and total phenolic compounds also were analyzed. In order to evaluate the Cr(VI) reduction potential of released pigments,

experiments were carried out by agitating 100 mL of 25 mg/L Cr(VI) solution along with 10 mL of pigment extract in a 250 mL conical flask. The solution was kept in a mechanical shaker at 150 rpm and the temperature was maintained at 30 °C. Samples were collected after 15, 30, 45, 60, 120 and 180 min of contact time. These samples were analyzed for residual concentration of Cr(VI), total chromium, tannin, total phenolic compounds and COD. All these studies were carried out at a pH of 7.0 ± 0.1.

2.6. Effect of ionic strength

In this experiments, kinetics of Cr(III) sorption by palm flower were compared at low (0 M NaCl) and high ionic strengths (0.1 M NaCl). The ionic strength of chromium solutions was adjusted using NaCl salt in the concentration range of 0–0.1 mol/L).

2.7. Column study

Fixed bed experiments were carried out in glass columns of 50 cm long and 1 cm internal diameter. The height of the packing media was 25 cm. The particle size of adsorbent used in the experiment was 400–500 μm. Synthetically prepared 20 mg/L of Cr(III) solution (pH 4.5) was trickled through the packed column, at a flow rate of 3 $m^3/(m^2\ h)$ (4.3 mL/min). These studies were conducted with and without organic matter (100 mg/L dextrose). To study the effect of bed height on biosorption, fixed bed studies were carried out with various bed depths of 5, 10, 15, 20 and 25 cm. For studying the reuse potential of the sorbent, the exhausted sorbent (5 g) was taken out and immersed in 100 mL of 5N H_2SO_4 and shaken at 150 rpm for 6 h, followed by washing thoroughly with distilled water until the wash water pH became neutral.

2.8. Analytical methods

COD analysis was carried out by closed reflux method as per standard procedure [24]. Cr(VI) concentration was determined by diphenyl carbazide method [24]. Total chromium concentration was analyzed using atomic absorption spectrometer (Perkin-Elmer, AAnalyst 700, USA). Cr(III) concentration was calculated by subtracting Cr(VI) concentration from total chromium concentration.

2.9. Fourier transform infrared (FT-IR) analysis

Infrared spectra of raw, treated and chromium-loaded biosorbents were obtained using a Fourier Transform Infrared spectrometer (Perkin-Elmer, USA). The Perkin-Elmer Spectrum One FTIR Spectrometer is capable of data collection over a wave number range of 450–4000 cm^{-1}. Adsorbents were dried in an oven at 60 °C for 24 h. For the FT-IR study, approximately 5 mg of finely ground sorbent was encapsulated in 1000 mg of KBr pellet (Sigma, USA) in order to prepare translucent sample disks.

3. Results and discussion

3.1. Kinetics of Cr(VI) and Cr(III) adsorption

The adsorption of trivalent chromium and hexavalent chromium by palm flower was initially evaluated in batch system, using 25 mg/L of chromium (Cr(VI) and Cr(III)) solution at a pH of 4.5 and a temperature of 30 °C. Fig. 1 shows the kinetics of Cr(III) and Cr(VI) sorption by *B. aethiopum*. From Fig. 1, it is clear that Cr(III) adsorption was higher (82.7%) and faster and attained equilibrium within 2 h whereas, Cr(VI) adsorption or disappearance was slower and even after 8 h (data not shown), equilibrium was not reached. In the experiments for Cr(VI) adsorption, to find whether Cr(VI) was getting converted to Cr(III) or it was being adsorbed, total chromium concentration in the system was also monitored. It is clear that only a part of Cr(VI) that disappeared from the system was adsorbed by palm flower and the remaining was present in the solution as Cr(III). The adsorption pattern of Cr(III) (expressed as total chromium) in this case was different from the adsorption of Cr(III) in the previous case. This may be due to the rate limitation of Cr(VI) reduction in the system.

3.2. Kinetics of Cr(VI) and Cr(III) adsorption by acid and alkali treated B. aethiopum

Bai and Abraham [10] reported that untreated adsorbent has less adsorption capacity, compared to chemically treated adsorbents, for chromium ions because the adsorbents lack appropriate chemical functional groups on its surface. Therefore, the adsorbent was subjected to alkali and acid treatments prior to biosorption studies. A weight loss of 18 and 49% was observed after acid and alkali treatments, respectively. This might be due to the removal of lignin and other compounds from the adsorbent under highly acidic and alkaline conditions.

The kinetics of biosorption of Cr(III) and Cr(VI) by the chemically treated adsorbent are presented in Fig. 2a. The pretreatment of biosorbents with 5N H_2SO_4 enhanced the Cr(VI) sorption whereas, there was a decrease in Cr(III) adsorption. It is apparent from Fig. 2a that only 62% Cr(III) removal was attained in 3 h by acid washed palm flower, however, 99.2% of Cr(VI) was removed from solution within 3 h. This could

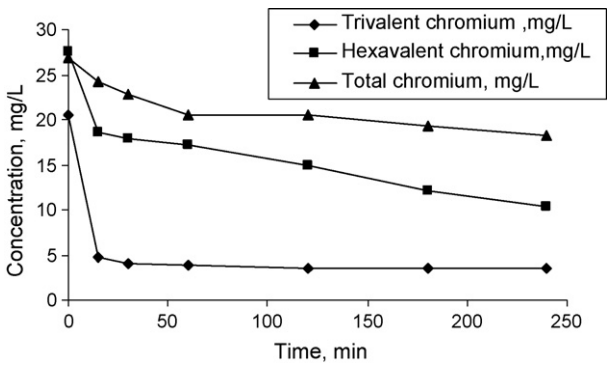

Fig. 1. Kinetics of Cr(VI) and Cr(III) adsorption by raw palm flower (*Borassus aethiopum*).

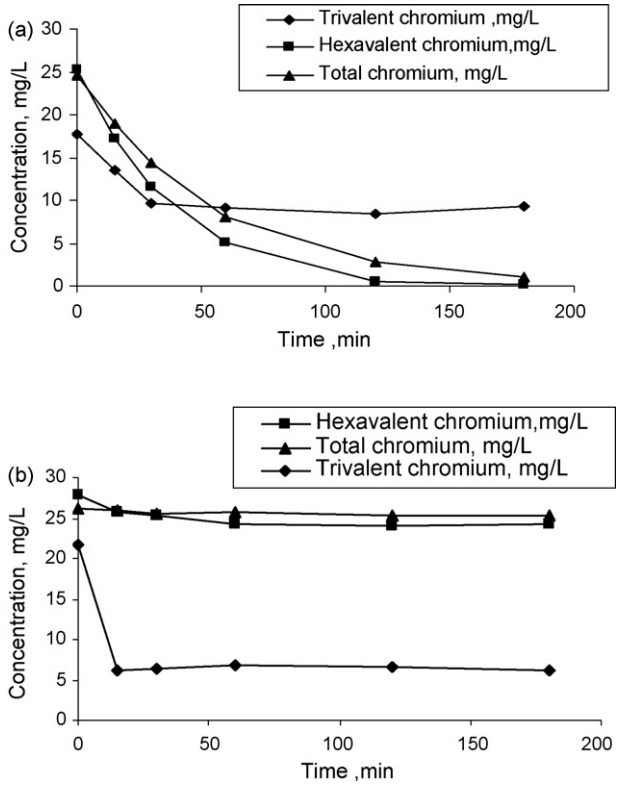

Fig. 2. (a) Kinetics of Cr(VI) and Cr(III) adsorption by acid treated palm flower (*B. aethiopum*); (b) kinetics of Cr(VI), total chromium and Cr(III) adsorption by alkali treated palm flower (*B. aethiopum*).

be attributed to the fact that acid hydrolysis yields relatively pure amino sugar, D-glucosamine [25], which is more easily protonated at adsorption pH. Thus extraction of finely powdered biosorbents in acids could expose more binding sites. Enhanced biosorption of metal ions by acid treated biosorbents have been reported while employing pine bark as adsorbent material [26,10]. Acid-treatment has increased the overall positive charge of the adsorbents. This was evident from the titration experiment with NaOH (data not shown). As a result, the sorbent was able to adsorb more negatively charged metal ions. However, the accessibility of cations might have decreased due to the decrease in sorption sites. For the pH range used in the present experiments (4.5–5.5), Cr(VI) ions exist in anionic form whereas, Cr(III) ions exist in cationic form [27]. It may also be noted that, after the acid wash, the organic matter content in the sorbent as well as in the reaction mixture was reduced (data not shown). This reduction resulted in a slower rate of Cr(VI) conversion to Cr(III). Hence, after the acid wash, a part of the Cr(VI) removal might be due to the adsorption of Cr(VI) directly to the biosorbent.

Treatment of the biosorbents with 4N NaOH significantly reduced the removal rate of Cr(VI) and total chromium (Fig. 2b). The Cr(III) adsorption capacity was not significantly reduced as compared to the raw adsorbent. This treatment also affected the physical characteristics of the adsorbent, thereby hindered the operational stability. There was drastic swelling of biosorbent, which may be due to the polymer chain breakage. The decrease in adsorption of Cr(VI) may be due to the net increase in the

Table 1
Adsorption rates constants obtained from pseudo-first-order model and pseudo-second-order model for palm flower

Nature of adsorbent	Chromium species	Pseudo-first-order model			Pseudo-second-order model			
		First-order reaction rate, k_1 (h^{-1})	q_e (mg/g)	R^2	Second-order reaction rate, k_2 ($g\,mg^{-1}\,h^{-1}$)	q_e (mg/g)	h ($mg\,g^{-1}\,h^{-1}$)	R^2
Raw	Trivalent chromium	7.258	1.696	0.924	0.321	1.706	0.935	1.000
	Hexavalent chromium	0.663	1.397	0.937	1.544	1.650	4.207	0.972
	Total chromium	0.626	1.349	0.976	2.095	0.879	1.618	0.988
Acid treated	Trivalent chromium	2.667	1.041	0.999	8.645	0.982	8.333	1.000
	Hexavalent chromium	2.106	2.824	0.997	0.379	3.447	4.498	0.997
	Total chromium	1.312	2.487	0.998	0.417	3.004	3.765	0.998

surface negative charge of the adsorbents or masking of surface groups by corresponding sodium salts.

3.3. Kinetic modeling of batch system

The rate of sorption onto a sorbent surface depends upon a number of parameters such as structural properties of the sorbent, initial concentrations of the solute, and the interaction between the solute and the active sites of the sorbent [28]. The effect of external film diffusion on biosorption rate is assumed to be insignificant and ignored in many kinetic analyses, particularly when the biosorbent is employed as a free suspension in a well-agitated batch system. To describe the adsorption process, kinetic data were fitted to Lagergren pseudo-first-order model and Ho's pseudo-second-order reaction rate model [29]. The mathematical representations of models are given in Eqs. (1) and (2), respectively,

$$\log(q_e - q_t) = \log q_e - k_1 t \quad (1)$$

$$\left(\frac{1}{q_t}\right) = \left(\frac{1}{h}\right) + \left(\frac{1}{q_t}\right) t \quad (2)$$

where q_e is the amount of adsorbate removed from aqueous solution at equilibrium, q_t is the amount of adsorbate sorbed on the sorbent surface at any time t, k is the rate constant of sorption, t is the reaction time and $h = k_2 q_e^2$.

Fig. 3b shows the second-order linear plot for acid washed *B. aethiopum*. The kinetic rate constants obtained from first- and second-order pseudo-kinetic model for both raw and acid treated biosorbents are given in Table 1. A larger adsorption rate constant k_1 usually represents quicker adsorption whereas a lesser k_2 value represents a faster adsorption [30]. For both Cr(VI) and Cr(III), the entire kinetic data fitted well with pseudo-second-order reaction rate model, which is evident from the higher correlation coefficient values.

Though the adsorption process is considered as a surface phenomenon, intra-particle diffusion also plays a significant role. Dubinin [31] suggested that pore size distribution plays a more significant role in adsorption process than surface area. For any adsorbent in an agitated system, main resistance to mass transfer occurs during the movement or diffusion of solute within the pores of the particles [32]. In order to test the contribution of intra-particle diffusion on adsorption process, the rate constant for intra-particle diffusion was calculated using the following equation [33]:

$$q_t = K_p t^{1/2} \quad (3)$$

For calculating K_p, a linear plot of q_t against square root of time ($t^{1/2}$) was made (Fig. 3c). The slope of the linear plot indicates the intra-particle diffusion rate constant. Table 2 shows the K_p value obtained for Cr(III), Cr(VI) and total chromium sorption by raw and acid treated *B. aethiopum*. The K_p value for Cr(III) was relatively higher compared to K_p value of Cr(VI) in case of raw adsorbent. However, the trend was reversed after acid washing. The linear portion of the curves (not shown) passed through the origin for all the cases. Therefore, it may be concluded that adsorption of chromium (Cr(III) and Cr(VI)) by palm flower is governed by intra-particle diffusion.

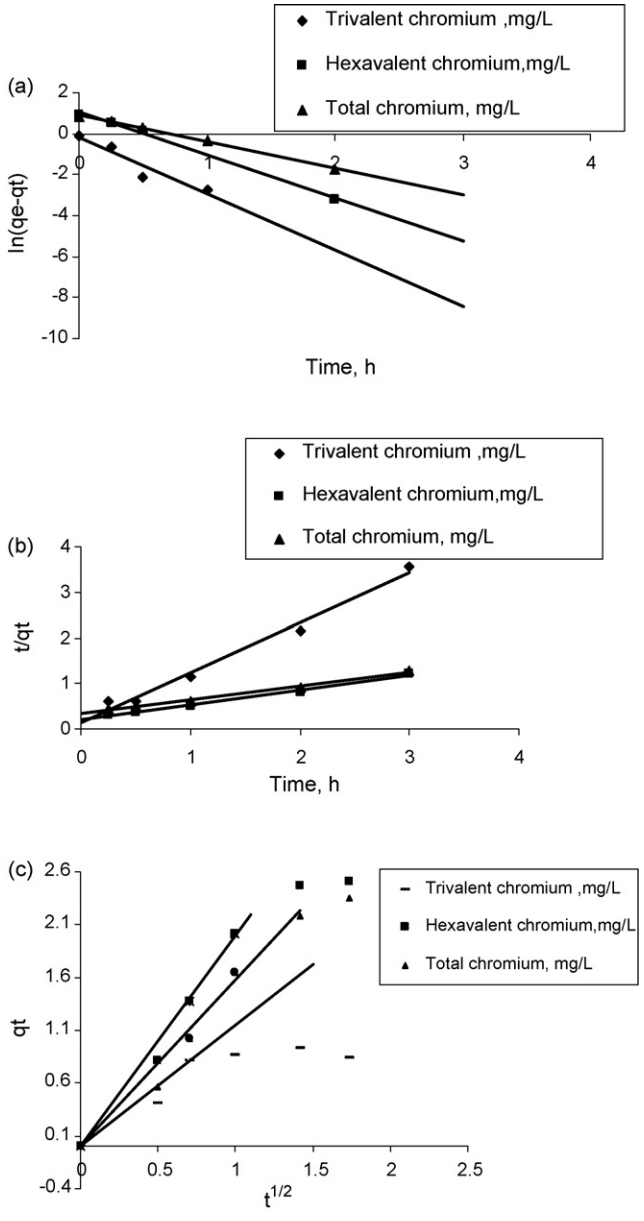

Fig. 3. (a) Pseudo-first-order kinetic model for chromium adsorption by acid treated palm flower; (b) pseudo-second-order kinetic model for chromium adsorption by acid treated palm flower; (c) intra-particle diffusion model for chromium adsorption by acid treated palm flower.

Table 2
Intra-particle mass transfer coefficients for raw and acid treated palm flower

Adsorbent	Chromium species	K_p (mg g^{-1} h$^{-1/2}$)	R^2
Raw	Trivalent chromium	3.167	1.000
	Hexavalent chromium	1.509	0.949
	Total chromium	0.570	0.993
Acid treated	Trivalent chromium	1.147	0.949
	Hexavalent chromium	1.994	0.999
	Total chromium	1.583	0.990

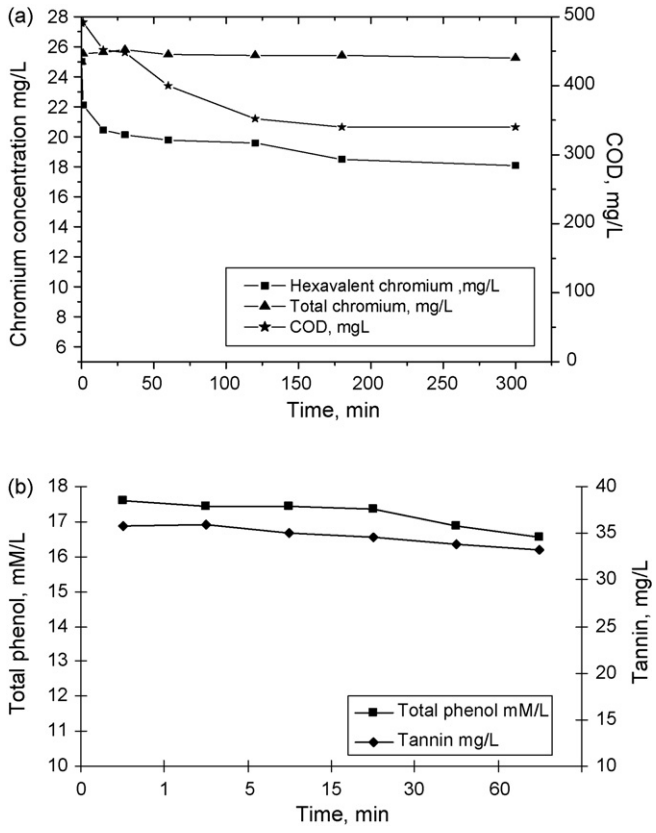

Fig. 4. (a) Kinetics of pigment release and Cr(VI) reduction by the released pigment from raw adsorbent; (b) kinetic of tannin and total phenol disappearance with respect to Cr(VI) reduction.

3.4. Role of released organic matter on Cr(VI) reduction

From the kinetic studies, it was clear that Cr(VI) removal from the system was due to the reduction of Cr(VI) to Cr(III) and subsequent adsorption of Cr(III) onto palm flower. It was noticed that during the adsorption process, significant amount of dissolved organic matter (480 mg/L as COD, Fig. 4) was released into the system. In order to find the role of organic matter released on Cr(VI) reduction, batch experiment was carried out using the released organic matter. The results are presented in Fig. 4. Cr(VI) reduction was very fast and about 25% of Cr(VI) was reduced in 15 min. Concentration of total chromium remained the same throughout the study. From this study, it is clear that the organic material released from palm flower had certain components which have high reduction potential unlike other organic matter. Jaysing and Philip [34] have reported that at high concentrations of glucose or molasses, there was no significant Cr(VI) reduction.

Table 4
Different sorption isotherm models used to predict the adsorbent capacity of palm flower

Isotherms	Expression	Parameter	References
Ferundlich	$q_e = K_F \times C_e^{1/n}$	K_F, n	[45]
Langmuir	$q_e = \frac{q_m \times b \times C_e}{1 + b \times C_e}$	q_m, b	[46]
Redlich–Peterson model	$q_e = \frac{K_r \times C_e}{1 + A_r C_e^{b_r}}$	K_r, A_r, b_r	[47]
Sips model	$q_e = \frac{q_m \times (K_s \times C_e)^{m_s}}{(1 + K_s C_e)^{m_s}}$	q_m, K_s, m_s	[48]
Radke–Prausmitz model	$q_e = \frac{K_{RP} \times q_m \times C_e}{(1 + K_{RP} \times C_e)^{m_{RP}}}$	K_{RP}, q_m, ^{m}RP	[49]
Toth model	$q_e = \frac{K_t \times C_e}{(A_t + C_e^t)^{1/t}}$	K_t, A_t, T	[50]

The characterization of organic material released from *B. aethiopum* using different eluents was carried out and the results are presented in Table 3. Concentration of tannin and total phenol was also estimated after the Cr(VI) reduction (Table 3). From these observations, it is evident that total phenol and tannin present in the system have a significant role in Cr(VI) reduction. It is reported that poly phenolic compounds can chelate metal ions *in vitro* [35]. While discussing the adsorption mechanism of hexavalent chromium by condensed tannin gel, Nakano et al. [36] described the etherification of chromate with tannin molecules, subsequent reduction of Cr(VI) to Cr(III), formation of carboxylic group by tannin molecules and ion exchange of Cr(III) by carboxyl/hydroxyl groups. Similar type of reaction might have taken place in the present system also.

3.5. Equilibrium studies

Many models have been proposed in the past to describe the equilibrium relationship between adsorbed and unadsorbed solutes. In this study, six adsorption models often reported in the literature, namely Freundlich (F), Langmuir (L), Redlich–Peterson (R–P), Radke–Prausnitz (RaP), Sips (S) and Toth (T), were tested to provide the best description of adsorption. The mathematical representations of these models are given in Table 4. In this, both F and L are two parameter models whereas the remaining four are three parameter models.

Freundlich and Langmuir isotherm parameters were calculated by linear form, while the other models were evaluated in their non-linear form. For the linear models, the coefficient of correlation (R^2) calculated based on least squares method was used for the assessment of isotherm accuracies whereas, for non-linear models, various constants were calculated by optimizing

Table 3
Estimation of tannin and total phenolic compounds leached out from palm flower

Sorbents	Tannin concentration			Total phenolic compounds	
	Distilled water (mg/g)	Phosphate buffer (100 mM) (mg/g)	Methanol (mg/g)	Distilled water (mM/g)	Methanol (mM/g)
Palm flower	20.56	15.44	7.41	15.66	19.73
Before Cr(VI) addition	17.92	–	–	8.79	–
After Cr(VI) addition	16.57	–	–	8.27	–

Table 5
Various adsorption isotherm constants for Cr(III) and Cr(VI) adsorption by raw and acid treated palm flower

Models	Parameter	Raw adsorbents			Acid washed adsorbents		
		Trivalent chromium	Hexavalent chromium		Trivalent chromium	Hexavalent chromium	
			Cr(VI)	Total Cr		Cr(VI)	Total Cr
Freundlich isotherm	K_f	3.042	0.342	0.032	0.228	2.541	1.907
	$1/n$	0.156	0.599	0.851	0.415	0.311	0.373
	RMSE	1.749	0.059	0.038	0.251	1.383	0.474
Langmuir isotherm	Q_m	5.995	4.888	3.803	1.408	7.138	7.657
	b	0.229	0.048	0.007	0.148	1.443	0.209
	RMSE	0.244	0.128	0.036	0.305	0.072	0.479
Redke–Prausnitz model	K_{rp}	0.158	0.046	0.005	10.5	3.381	0.310
	q_m	6.227	4.610	4.183	0.057	5.212	4.753
	m_{rp}	1	0.945	0.707	0.531	0.935	0.810
	RMSE	0.2871	0.022	0.008	0.0392	0.018	0.076
Toth model	K_t	5.406	4.933	4.010	1.311	7.408	7.084
	A_t	144.43	28.472	588.621	136	0.437	21.906
	T	2.501	1.052	1.215	10	0.666	1.550
	RMSE	0.0527	0.004	0.002	0.2406	0.021	0.093
Redlich–Peterson model	A	0.975	0.386	0.080	0.611	18.492	0.984
	B	0.123	0.193	30.477	3.241	3.437	0.092
	g	1.137	0.678	0.177	0.635	0.942	1.207
	RMSE	0.0121	0.044	0.104	0.1507	0.019	0.039
Sips	q_m	5.481	4.575	3.714	4.716	7.272	7.151
	k_s	0.263	0.051	0.008	0	1.592	0.207
	m_s	1.696	1.048	1.140	0.12	0.766	1.364
	RMSE	0.0909	0.090	0.010	0.0177	0.023	0.005

the sum of the squares of the errors using the *solver* add-in from Microsoft's spreadsheet, Excel®. The isotherm accuracies were determined by root mean square error method.

The root mean squared error (RMSE) of a model is evaluated by Eq. (4):

$$\mathrm{RMSE} = \sqrt{\frac{1}{n}\sum_{i=1}^{n}(P_i - T_i)^2} \quad (4)$$

where P_i is the predicted value and T_i is the target value for fitness cases i.

The isotherm constants obtained from all the above-mentioned models are presented in Table 5. It is clear from the results that the adsorption data is fitting well for almost all the models. Neither two parameter models nor three parameter models showed any added advantage. For Cr(III), maximum specific adsorption capacity obtained were 5.99 mg/g (L), 6.27 mg/g (R–P), 5.406 mg/g (T) and 5.481 mg/g (S), respectively. Their corresponding linear and non-linear isotherms are illustrated in Fig. 5a. For Cr(VI), maximum adsorption capacity calculated were 4.98 mg/g (L), 3.57 mg/g (R–P), 4.933 mg/g (T) and 5.366 (S). Their corresponding isotherm plots are illustrated in Fig. 5b. For the same experiment, the total chromium removal was also evaluated. As shown in Table 5 and Fig. 5c, removal of total chromium was significantly lower than that of Cr(VI). This clearly shows that Cr(VI) was getting reduced to Cr(III) and a part of it was adsorbed by the sorbents.

Sorption equilibrium studies were also conducted with acid treated biosorbent (Table 5). As expected, the adsorption capacity of acid washed adsorbent for Cr(III) was less compared to the raw adsorbent. However, there was a significant increase in adsorption capacity in case of Cr(VI), after the acid treatment. The Cr(VI) adsorption capacity for acid treated adsorbent were 7.138 mg/g (L), 7.408 (T) mg/g and 7.272 (S) and 7.657 mg/g(L), 7.08 (T) mg/g and 7.151 (S) based on Cr(VI) and total chromium measurements, respectively. Generally, acid-treatment is being used for cleaning the cell wall and replacing the natural mix of ionic species bound on the cell wall with protons and sulfates [37–39]. Acid-treatment might have increased the exposed positive sites (protonation of functional groups like carboxyl and amino groups) on the adsorbents. The amino, carboxyl, nitrogen and oxygen of the peptide bonds, can be available in the adsorbent for characteristic coordination bonding with metallic ions [40]. Thus, acid-treatment might have exposed more binding sites; and therefore, the sorption capacity of the anionic Cr(VI) might have increased. As discussed earlier, at pH 4.5–5.5. Cr(VI) exists in anionic form whereas, Cr(III) preferably exists in cationic form. This must be the reason for higher adsorption of Cr(VI) and lower adsorption of Cr(III) by the acid treated adsorbents.

3.6. Regeneration and reuse studies

For the sustainability of adsorption process, the adsorbents should have good desorption and reuse potential. Studies were

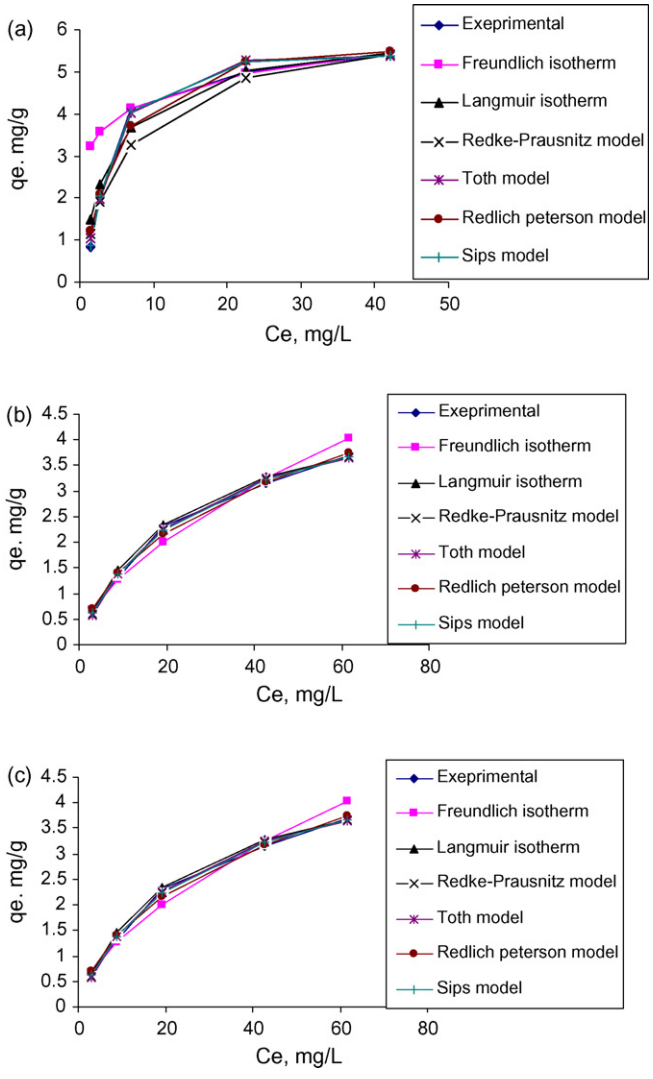

Fig. 5. (a) Predicted and experimental equilibrium adsorption curves for Cr(III) by palm flower; (b) predicted and experimental equilibrium adsorption curves for Cr(VI) by palm flower; (c) predicted and experimental equilibrium adsorption curves for total chromium by palm flower.

carried out to evaluate the reuse potential of palm flower as an adsorbent for chromium. Strong acid and alkali were used for this purpose. Repeated acid treatment has reduced the weight of adsorbent considerably. As shown in Fig. 6a, there was approximately 17% weight loss in the first acid wash and a total of 37% of the weight was lost in the second wash with 5N H_2SO_4. However, there was no significant weight loss after the second wash. This shows that, in the first two cycles, almost all acid soluble material from the biosorbent was washed away and the left over material was acid resistant. The kinetics of Cr(III), Cr(VI) and total chromium removal by the regenerated biosorbent is presented in Fig. 6b, d and e. Cr(III) adsorption was reducing as the number of recycles progressed. However, Cr(VI) adsorption capacity increased as the number of regeneration increased. As seen in the earlier kinetic studies with raw and acid washed adsorbents, Cr(III) adsorption was adversely affected by acid treatment whereas it significantly increased in the case of Cr(VI).

Fig. 6c–f shows the kinetics of Cr(III) desorption in different cycles of operation. The percentage desorption of Cr(III) was 74.7%, 84.1% and 96.8% in first, second and third cycles of operation. The lower desorption in the first cycle may be the irreversible adsorption of Cr(III) to some of the functional groups. As the acid washing proceeded, these material must have washed away (evident from weight loss) and Cr(III) adsorption in the remaining functional groups might be reversible. The changes in functional groups on the adsorbent surfaces were clear during FT-IR analysis.

3.7. Effect of ionic strength

Effect of ionic strength on Cr(III) sorption by raw and acid treated adsorbents are shown in Fig. 7a and b. It is clear from the figures that Cr(III) removal was slightly decreased with increase in ionic strength. In general, adsorption decreases with increasing ionic strength of the aqueous solution [41,42].

3.8. Fourier transform infrared (FT-IR) analysis of adsorbents

The FT-IR spectrum of raw and acid and alkali treated adsorbents before and after sorption of both hexavalent and trivalent chromium were used to determine the vibration frequency changes in the functional groups, in the adsorbents. The spectra of adsorbents were measured within the range of 400–4000 cm^{-1} wave number. The FT-IR spectrum of palm flower displays a number of absorption peaks, indicating the complex nature of the biosorbent (Fig. 8a).

The broad absorption peak around 3403 cm^{-1} is indicative of the existence of –OH and –NH stretching, thus showing the presence of hydroxyl and amine groups on the adsorbent. The band at 2925 cm^{-1} can be assigned to the –CH stretch. The absorption bands at 1623 cm^{-1} (mainly C=O stretch) and 1498 cm^{-1} (mainly –NH stretch) can be attributed to the I and II bands of amide bond in the protein peptide bond. It was clear that the carboxylate ions gave rise to two bands: C=O stretch at 1378 and 1707 cm^{-1}. A band at about 1118 cm^{-1}, representing $–SO_3$ stretching, was also observed in the FT-IR spectrum of palm flower.

Significant changes of the functional group are visible after acid treatment. Acid treatment has been used for cleaning the cell wall and replacing the natural mix of ionic species bound on the cell wall with protons and sulfates [37–39]. Results (Fig. 8a) show the changes in functional group, i.e. carboxylic acids in 1709 cm^{-1}, esters in 1294 cm^{-1}, amides in 1623 cm^{-1} and amines in 2320 cm^{-1} in acid washed adsorbent compared to the raw one. The acid hydrolysis converts amide and ester groups in to corresponding carboxylic acids [43]. The hydrolyzing esters—splitting them into carboxylic acids (or their salts) and alcohols by the action of water, dilute acid or dilute alkali. Acid hydrolyze amides to produce carboxylic acid and amine [43]. The observed peaks at 1551 cm^{-1} and 804 cm^{-1} represent the increased intensity of primary and secondary amine.

Treatment of the biosorbents with 4N NaOH significantly reduced the adsorption capacity, as discussed earlier. FT-IR spec-

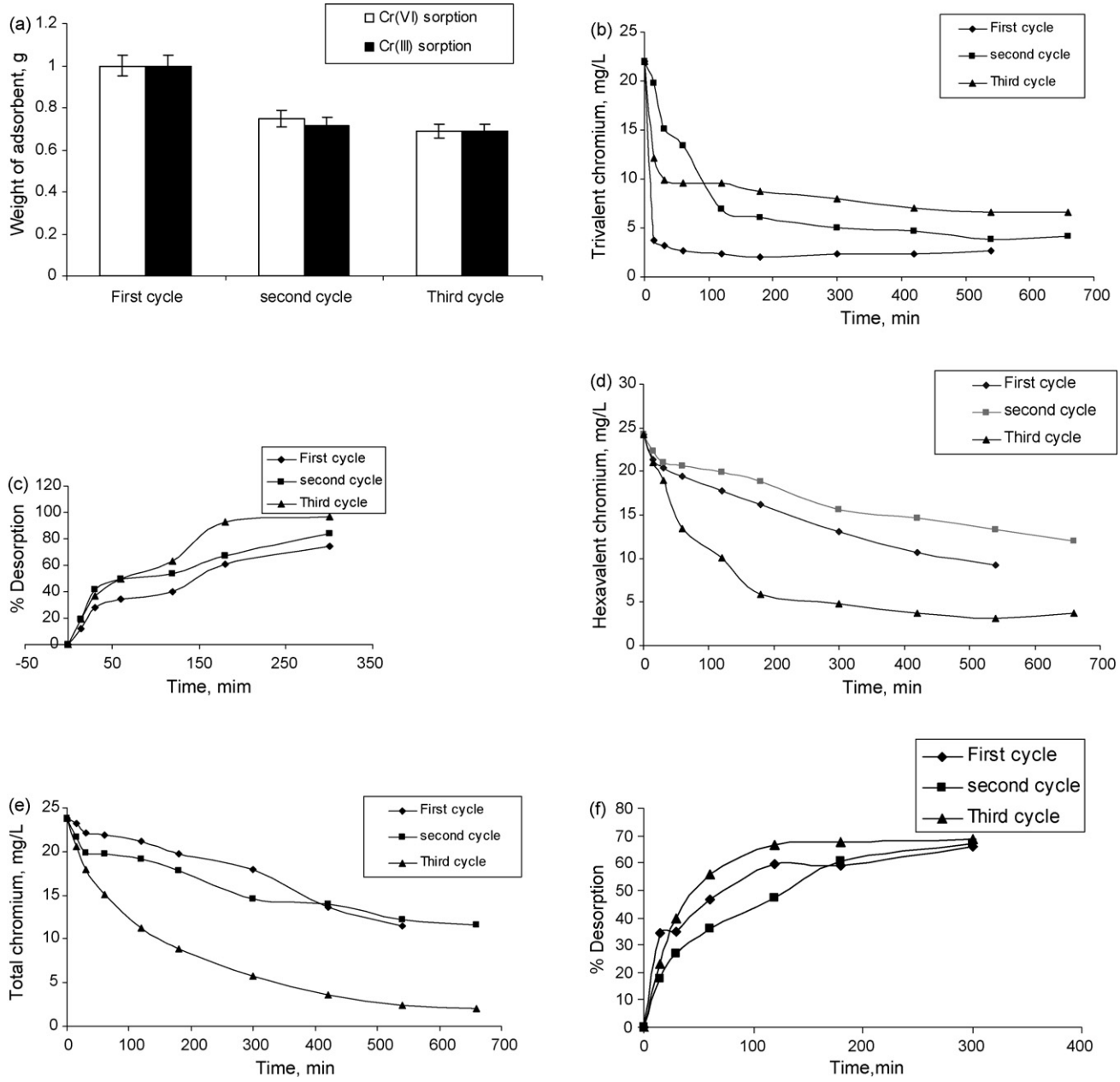

Fig. 6. (a) Weight losses due to acid (5N H_2SO_4) wash in different cycles; (b) kinetics of Cr(III) adsorption by palm flower at different cycles; (c) kinetics of Cr(III) desorption from palm flower at different cycle; (d) kinetics of Cr(VI) adsorption by palm flower at different cycle; (e) kinetics of total chromium adsorption by palm flower at different cycle; (f) kinetics of Cr(VI) desorption from palm flower at different cycle.

trum of alkali treated palm flower is given in Fig. 8a. There were significant functional group changes after the alkali wash. The changes are visible for carboxylic acids in 1710 cm^{-1}, esters in 1250 cm^{-1}, amides in 1625 cm^{-1} and amines in 2309 cm^{-1}. Alkali treatment might have formed corresponding metal salts with functional groups on the adsorbent. Observed peaks at 1709 cm^{-1}, 749 cm^{-1} and 1531 cm^{-1} represent the decreased intensity of carboxylic acids, and amide groups. The peak at 1196 cm^{-1} shows the increased intensity of tertiary alcohol.

Change in functional group are observed after Cr(VI) adsorption (Fig. 8b). Cr(VI) is a powerful oxidizing agent, which might have oxidized primary and secondary alcohols to corresponding ketones, carboxylic acids and other compounds having "benzyl" hydrogen to benzoic acids, and Cr(VI) got reduced to Cr(III). The peaks at 1731 cm^{-1}, 1709 cm^{-1}, 749 cm^{-1} and 1531 cm^{-1} represent the decreased intensity of ketone, carboxylic acids, amide and amine groups.

To confirm the difference in functional groups after the biosorption of Cr(III), FT-IR study was carried out using Cr(III)-loaded adsorbent. The absorption spectrum of chromium-loaded adsorbent (at pH 4.5) was compared with that of raw palm flower. A change of absorption bands can be seen when comparing the FT-IR spectra of pristine and chromium-loaded biosorbent Fig. 8c. An interesting phenomenon was the sharp decrease in the band intensity at 1400 cm^{-1} corresponding to C=O stretching after metal binding. Although, slight changes in other absorp-

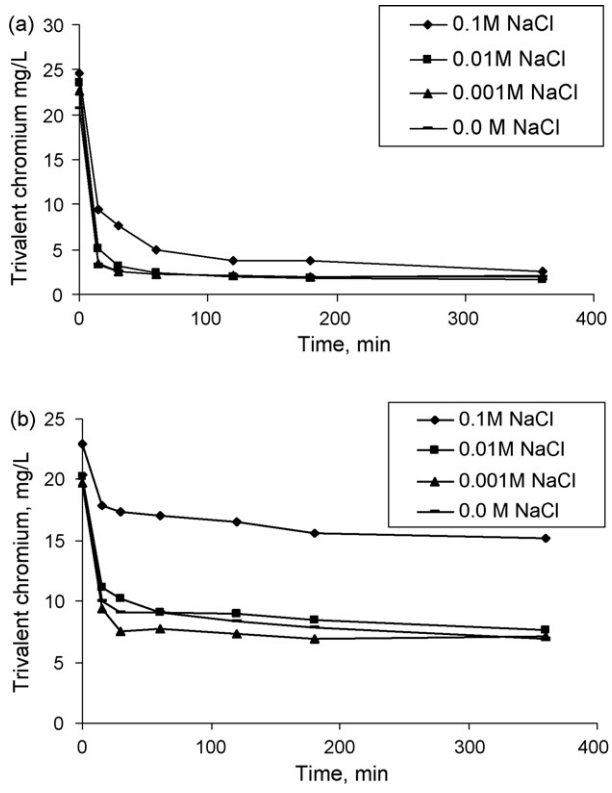

Fig. 7. (a) Effect of ionic strength on the adsorption of Cr(III) by raw palm flower (*B. aethiopum*) at pH 4.5; (b) effect of ionic strength for adsorption of Cr(III) on acid treated palm flower (*B. aethiopum*) at pH 4.5.

tion frequencies were observed, it was difficult to interpret how these absorption peaks were related to Cr(III) biosorption.

3.9. Column studies

The breakthrough time and the shape of the breakthrough curve are important characteristics for determining the operation and the dynamic response of an adsorption column. The breakthrough curves of Cr(III) adsorption by palm flower at a flow rate of 4.3 mL min^{-1} and a fixed bed height of 25 cm are shown in Fig. 9a. Slightly earlier breakthrough was observed in the case of Cr(III) with organic matter compared to Cr(III) alone. Cr(III) uptake capacity of 5.878 mg/g was obtained when the column was challenged with synthetic Cr(III) solution. Presence of organic matter (100 mg/L of COD) along with Cr(III), marginally reduced the uptake capacity of sorbent (5.754 mg/g). From the adsorption capacity, it is evident that addition of low concentrations of organic matter has insignificant effect on column performance.

The sorption data evaluated based on a number of regeneration reuse cycles are presented in Table 6. The column exhibited maximum Cr(III) adsorption capacity in the first cycle (Fig. 9b). In the second cycle, after the regeneration with 200 mL of 5N H_2SO_4, there was a weight loss of 33%. The adsorption capacity reduced to 3.71 mg/g which corresponds to a reduction of 35.5%. As observed in the batch studies, acid treatment has

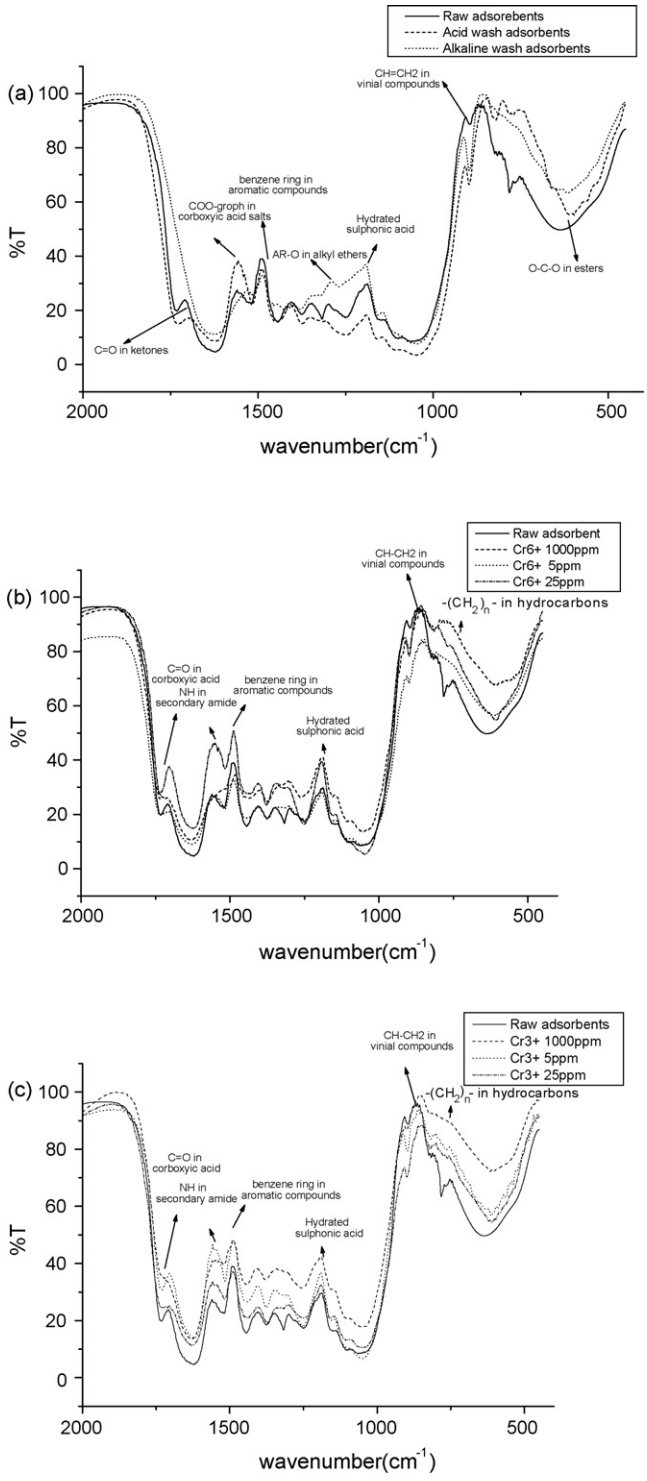

Fig. 8. (a) FT-IR of raw, acid treated, and alkali treated adsorbents; (b) FT-IR of hexavalent chromium-loaded adsorbents; (c) FT-IR of trivalent chromium-loaded adsorbent.

adverse effect on Cr(III) uptake. This may be the reason for the reduction in Cr(III) uptake by the regenerated adsorbent. Third cycle of operation has given almost same performance as the second cycle (3.62 mg/g). This shows that the sites responsible for Cr(III) adsorption after acid wash are reversible and the adsorbent can be utilized for a number of times without

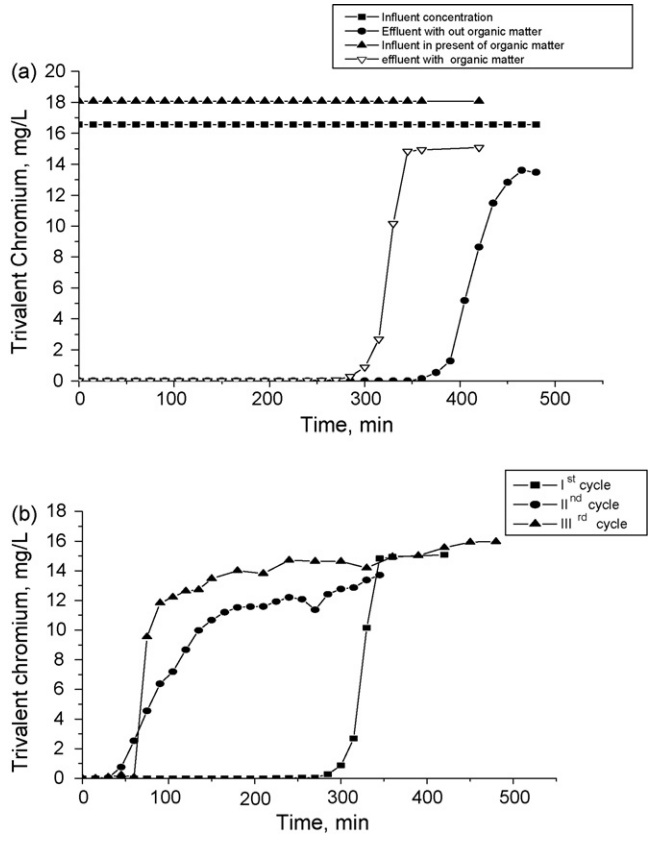

Fig. 9. (a) Break through curve of Cr(III) in presence and absences of organic matter (flow rate = 4.3 mL/min, initial bed depth = 25cm and pH 4.5); (b) reuse potential of fixed bed columns (flow rate = 4.3 mL/min, initial Cr(III) concentration = 16.56 mg/L, COD = 100 mg/L, initial bed depth = 25 cm and pH 4.5).

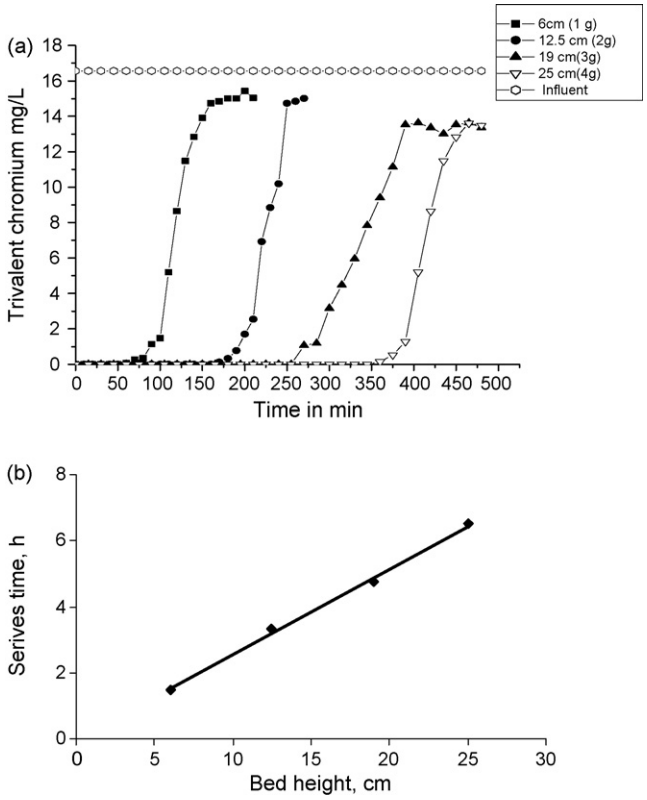

Fig. 10. (a) Breakthrough curves for Cr(III) using palm flower as adsorbent: Effect of bed heights (flow rate = 4.3 mL/min, initial Cr(III) concentration = 16.56 mg/L, COD = 0 mg/L and pH 4.5); (b) BDST model plot for Cr(III) biosorption by palm flower (flow rate = 4.3 mL/min, initial concentration = 16.6 mg/L, pH 4.5).

much reduction in the efficiency. Based on the batch desorption and reuse study results, this biosorbent may exhibit better results in successive cycles after regeneration in case of Cr(VI) adsorption.

3.10. Modeling of the continuous system

The Bed Depth Service Time (BDST) model, proposed by Bohart and Adams [44] is based on physically measuring the capacity of the bed at different breakthrough values. The BDST model states that bed height (Z) and service time (t) of a column bears a linear relationship. The equation can be expressed as

$$t = \frac{N_0 \times Z}{C_0 V} - \frac{1}{K_a C_0} \ln\left(\frac{C_0}{C_b} - 1\right) \quad (5)$$

The parameters N_0 and K_a can be calculated from the slope of the linear plot of t_b versus Z.

Fig. 10a shows the breakthrough curves of Cr(III) adsorption onto palm flower at different bed depths (6, 12, 19 and 25 cm). The column service time was selected as the time when the effluent Cr(III) concentration reached 1 mg/L, which is the permissible discharge standard as per Bureau of Indian Standards (BIS). The plot of service time against bed height at a flow rate of 4.3 mL/min (Fig. 10b) was linear ($R^2 = 0.9971$), indicating the validity of BDST model for the present system. The computed N_0 and K_a were 1284 mg/L and 9.98 L/mg h, respectively. If K_a is large, even a short adsorbent bed can avoid breakthrough, but as K_a decreases, a progressively longer adsorbent bed is required to avoid the breakthrough. The BDST model parameters can be useful to scale up the process for other flow rates without further experiments.

Table 6
Adsorption capacity of palm flower in various regeneration and reuse cycles

Cycle of operation	% Weight loss from original value (taken 4.5 g adsorbent)		Adsorption	
	Weight (g)	% Loss	Capacity (mg/g)	% Reduction adsorption capacity
First cycle	2.84	36.7	5.754	100
Second cycle	2.59	8.76	3.709	64.45
Third cycle	2.55	1.54	3.62	62.91

Studies were conducts in presence of 100 mg/L COD and desorption with 100 mL of 5N H_2SO_4.

4. Conclusions

Batch kinetic and equilibrium experiments were conducted to determine the trivalent and hexavalent chromium adsorption rate and adsorption capacities of palm flower (male). The adsorption was a very fast process and in most of the cases, adsorption followed second-order kinetics. In case of Cr(VI) adsorption, first it was reduced to Cr(III) with the help of tannin and phenolic compounds and subsequently got adsorbed. Adsorption equilibrium data was fitting well with most of the well-known models. Acid treatment significantly increased the Cr(VI) adsorption capacity of palm flower. However, there was a reduction in Cr(III) adsorption capacity by the acid washed adsorbents. Alkali treatment reduced the adsorption capacity of palm flower for both Cr(III) and Cr(VI). Regeneration studies were carried out to evaluate the reuse potential of the biosorbent. FT-IR spectrum showed the functional group changes during adsorption of Cr(III) and Cr(VI). Column studies were conducted to generate the information for scale-up of the process.

References

[1] I.B. Singh, D.R. Singh, Cr(VI) removal in acidic aqueous solution using iron-bearing industrial solid wastes, their stabilization with cement, Environ. Technol. 23 (2002) 85–95.
[2] D.C. Sharma, C.F. Forster, A preliminary examination into the adsorption of hexavalent chromium using low-cost adsorbents, Biores. Technol. 47 (1994) 257–264.
[3] V. Sarin, K.K. Pant, Removal of chromium from industrial waste by using eucalyptus bark, Bioresour. Technol. 97 (2006) 15–20.
[4] S. Ricordel, S. Taha, I. Cisse, G. Dorange, Heavy metals removal by adsorption onto peanut husks carbon: characterization, kinetic study and modeling, Sep. Purif. Technol. 24 (2001) 389–401.
[5] G. Selvakumari, M. Murugesan, S. Pattabi, M. Sathishkumar, Treatment of electroplating industry effluent using maize cob carbon, Bull. Environ. Contam. Toxicol. 69 (2001) 195–222.
[6] F. Kargi, S. Cikla, Determination of model parameters for zinc(II) ion biosorption onto powdered waste sludge (PWS) in a fed-batch system, J. Environ. Manage. 85 (2007) 883–890.
[7] A.J. Rapoport, O.A. Muter, Biosorption of hexavalent chromium by yeast, Process Biochem. 30 (1995) 145–149.
[8] R. Sudha Bai, T.E. Abraham, Biosorption of Cr(VI) from aqueous solution by *Rhizopus nigrificans*, Bioresour. Technol. 79 (2001) 73–81.
[9] T. Verma, T. Srinath, P. Ramteke, S. Garg, Chromium(VI) biosorption and bioaccumulation by chromate resistant bacteria, Chemosphere 48 (2002) 427–435.
[10] R. Sudha Bai, T. Emilia Abraham, Studies on enhancement of Cr(VI) biosorption by chemically modified biomass of *Rhizopus nigricans*, Water Res. 36 (2002) 1224–1236.
[11] N. Goyal, S.C. Jain, U.C. Banerjee, Comparative studies on microbial adsorption of heavy metals, Adv. Environ. Res. 7 (2003) 235–250.
[12] R. Sudha Bai, T. Emilia Abraham, Studies on chromium(VI) adsorption desorption using immobilized fungal biomass, Bioresour. Technol. 87 (2003) 17–26.
[13] V.K. Gupta, A.K. Shrivastava, N. Jain, Biosorption of chromium(VI) from aqueous solution by green algae *Spirogyra* species, Water Res. 35 (2001) 4079–4085.
[14] H. Ucun, Y.K. Bayhan, Y. Kaya, O.F. Algur, Biosorption of chromium(VI) from aqueous solution by cone biomass of *Pinus sylvestris*, Bioresour. Technol. 85 (2002) 155–158.
[15] K. Chandra Sekhar, C.T. Kamala, N.S. Chary, Y. Anjaneyulu, Removal of heavy metals using a plant biomass with reference to environmental control, Int. J. Miner. Process. 68 (2003) 37–45.
[16] S.E. Bailey, T.J. Olin, R.M. Bricka, D.D. Adrian, A review of potentially low-cost sorbents for heavy metals, Water Res. 33 (1999) 2469–2479.
[17] F.N. Acar, E. Malkoc, The removal of chromium(VI) from aqueous solutions by *Fagus orientalis* L., Bioresour. Technol. 94 (2004) 13–15.
[18] K. Vijayaraghavan, J. Jegan, K. Palanivelu, M. Velan, Biosorption of cobalt(II) and nickel(II) by seaweeds: batch and column studies, Sep. Purif. Technol. 44 (2005) 53–59.
[19] K. Kadirvelu, K. Thamaraiselvi, C. Namasivayam, Adsorption of nickel(II) from aqueous solution onto activated carbon prepared from coir pith, Sep. Purif. Technol. 24 (2001) 497–505.
[20] W.T. Tan, S.T. Ooi, C.K. Lee, Removal of Cr(VI) from solution by coconut husk, palm pressed fibers, Environ. Technol. 14 (1993) 277–282.
[21] J. Romero González, J.R. Peralta Videa, E. Rodríguez, M. Delgado, J.L. Gardea Torresdey, Potential of *Agave lechuguilla* biomass for Cr(III) removal from aqueous solutions: thermodynamic studies, Bioresour. Technol. 97 (2006) 178–182.
[22] D. Park, Y.S. Yun, H.Y. Cho, J.M. Park, Chromium biosorption by thermally treated biomass of the brown seaweed, *Ecklonia* sp., Ind. Eng. Chem. Res. 43 (2004) 8226–8232.
[23] J. Romero González, J.R. Peralta-Videa, E. Rodríguez, S.L. Ramirez, J.L. Gardea Torresdey, Determination of thermodynamic parameters of Cr(VI) adsorption from aqueous solution onto *Agave lechuguilla* biomass, J. Chem. Thermodyn. 37 (2005) 343–347.
[24] APHA, AWWA, WPCF, Standard Methods for the Examination of Water and Wastewater, 20th ed., American Public Health Association, Washington, DC, 1998.
[25] R.K.G. Nair, P. Madhavan, Chitin, chitosan and their derivatives, production and applications, in: Proceedings of the VIIIth Carbohydrate Conference, Trivandrum, November 18–20, 1992, pp. 59–65.
[26] L. Teles, A.de. Vasconcelos, C.G. Gonzalez Beca, Chemical activation of pine bark to its adsorption capacity of metal ions. Part I. By acid treatment, Eur. Water Pollut. Control 7 (1997) 41–46.
[27] K. Rama Krishna, L. Philip, Bioremediation of Cr(VI) in contaminated soils, J. Hazard. Mater. 121 (2005) 109–117.
[28] E.A. Oliveira, S.F. Montanher, A.D. Andrade, J.A. Nóbrega, M.C. Rollemberg, Equilibrium studies for the sorption of chromium and nickel from aqueous solutions using raw rice bran, Process Biochem. 40 (2005) 3485–3490.
[29] Y.S. Ho, G. McKay, Pseudo-second order model for sorption processes, Process Biochem. 34 (1999) 451–465.
[30] M.M. Shihabudheen, K.S. Atul, P. Ligy, Manganese-oxide-coated alumina: a promising sorbent for defluoridation of water, Water Res. 40 (2006) 3497–3506.
[31] M.M. Dubinin, Adsorption in micropores, J. Coll. Interface Sci. 23 (1967) 487–499.
[32] S.J. Allen, G. McKay, K.Y.H. Khader, Equilibrium adsorption isotherms for basic dyes onto lignite, J. Chem. Technol. Biotechnol. 45 (1989) 291–302.
[33] W.J. Weber, J.C. Morris, Advances in water pollution research: removal of biologically resistant pollutants from waste waters by adsorption, in: Proceedings of the International Conference on Water Pollution Symposium, vol. 2, Pergamon, Oxford, 1962, pp. 231–266.
[34] J. Jeyasingh, L. Philip, Bioremediation of chromium contaminated soil: optimization of operating parameters under laboratory conditions, J. Hazard. Mater. 118 (2005) 113–120.
[35] N. Lavid, A. Schwartz, O. Yarden, E. Tel-Or, The involvement of polyphenols and peroxidase activities in heavy metal accumulation by epidermal glands of the water lily (Nymphaeaceae), Planta 212 (2001) 323–331.
[36] Y. Nakano, K. Takeshita, T. Tsutsumi, Desorption mechanism of hexavalent chromium by redox within condensed tannin gel, Water Res. 35 (2001) 496–500.
[37] Y.S. Yun, D. Park, J.M. Park, B. Volesky, Biosorption of trivalent chromium on the brown seaweed biomass, Environ. Sci. Technol. 35 (2001) 4353–4358.
[38] T.A. Davis, B. Volesky, A. Mucci, A review of the biochemistry of heavy metal biosorption by brown algae, Water Res. 37 (2003) 4311–4330.

[39] Y.S. Yun, Characterization of functional groups of protonated *Sargassum polycystum* biomass capable of binding protons and metal ions, J. Microbiol. Biotechnol. 14 (2004) 29–34.
[40] H. Niu, B. Volesky, Characteristics of anionic metal species biosorption with waste crab shells, Hydrometallurgy 71 (2003) 209–215.
[41] D. Donmez, Z. Aksu, Removal of chromium(VI) from saline wastewaters by *Dunaliella* species, Process Biochem. 38 (5) (2002) 751–762.
[42] G.S. Agarwal, H.K. Bhuptawat, S. Chaudhari, Biosorption of aqueous chromium(VI) by *Tamarindus indica* seeds, Bioresour. Technol. 99 (7) (2006) 949–956.
[43] Milos Hudlicky, Reductions in Organic Chemistry, Ellis Horwood Limited, New York, 1984.
[44] G.S. Bohart, E.Q. Adams, Behaviour of charcoal towards chlorine, J. Chem. Soc. 42 (1920) 523–529.
[45] H.M.F. Freundlich, Über die adsorption in Lösungen, Z. Phys. Chem. 57 (1906) 385–470.
[46] Langmuir, The adsorption of gases on plane surface of glass, mica and platinum, J. Am. Chem. Soc. 40 (1916) 1361–1403.
[47] C.J. Radke, J.M. Prausnitz, Adsorption of organic solutes from dilute aqueous solutions on activated carbon, Ind. Eng. Chem. Fundam. 11 (1972) 445–450.
[48] R. Sips, Structure of a catalyst surface, J. Chem. Phys. 16 (1948) 490–495.
[49] O. Redlich, C. Peterson, Useful adsorption isotherm, J. Phys. Chem. 63 (1958) 1024.
[50] J. Toth, State equations of the solid gas interface layer, Acta Chem. Acad. Hung. 69 (1971) 311–317.